Impact of microphysics on tropical precipitation extremes in a global storm-resolving model

Jiawei Bao[1], Julia M. Windmiller[1]

[1]Max Planck Institute for Meteorology, Hamburg, Germany

Key Points:

- Changes in microphysics influence tropical precipitation extremes in a global storm-resolving model.
- Hourly precipitation extremes are influenced dynamically through convective updraft speed, which depends on the raindrop terminal velocity.
- Daily precipitation extremes are more sensitive to the microphysical modulation on convective organization.

Corresponding author: Jiawei Bao, `jiawei.bao@mpimet.mpg.de`

Abstract

The impact of microphysics on tropical precipitation extremes is explored with a global storm-resolving model by modifying the terminal velocity of raindrops. Depending on the time scales, precipitation extremes respond differently. Hourly extremes are influenced dynamically through convective updraft speed, as a faster terminal velocity of raindrops increases the updraft speed by reducing the total rain in the atmosphere which increases the updraft buoyancy. However, the response of daily precipitation extremes is more sensitive to the microphysical modulation on convective organization. By being more organized with decreasing terminal velocity, daily precipitation extremes are enhanced due to increased precipitation efficiency and intensified updrafts. Thus, the results suggest that microphysics, despite often occurring at small scales, can influence the circulation at larger scales, and the microphysical imprint across different scales plays an important role in regulating tropical precipitation extremes.

Plain Language Summary

We use a global high-resolution climate model to explore the response of tropical extreme precipitation to processes governing the rain formation. We artificially alter the fall speed of raindrops to investigate its impact. The results show that it not only affects local short-duration precipitation extremes by changing the updraft speed, but also has the ability to modulate the spatial distributions of precipitation, which in the end influences precipitation extremes accumulated over longer time scales.

1 Introduction

Precipitation extremes have long been posing tremendous threats to our society, and global warming adds extra uncertainties and likely exacerbates the situation. The uncertainties come partially from the variable nature of the extremes. Unlike mean precipitation which is constrained energetically (Allen & Ingram, 2002; Held & Soden, 2006), extreme precipitation, occurring at small scales, can be sensitive to many local influences (O'Gorman, 2015) and, therefore, is much less known.

The conventional climate models generally struggle to simulate extremes, and cannot reach a consensus in terms of how the tropical daily precipitation extremes respond to climate change (O'Gorman & Schneider, 2009). The disagreement comes primarily from the inconsistencies in convective updraft speed, which is attributed to the model deficiency to represent convective processes due to the coarse model resolution (typically at $100\,\mathrm{km}$) and the use of convective parameterization. Because of the model deficiencies in parameterized convection, the impact from the microphysics is often obscured.

In recent decades, with computational and technological advances, it has become feasible to run simulations at a resolution ($\leq 5\,\mathrm{km}$) at which convective parameterization can be switched off. Such high-resolution simulations are, however, often restricted to be over relatively small domains instead of the entire globe. Nevertheless, progress has been made in understanding tropical precipitation extremes. One important finding is the recognition of the microphysical changes in modulating precipitation extremes. Using idealized simulations configured in radiative-convective equilibrium (RCE) without rotation, Parodi and Emanuel (2009) found that the terminal velocity of raindrops determines the convective updraft speed through the condensate loading effect, which acts, dynamically, to alter precipitation extremes. With a similar setup, Singh and O'Gorman (2014) found that the response of extreme precipitation to warming depends on the choice of microphysics scheme, and that this dependency mainly comes from the effective hydrometeor fall speed simulated by different schemes which affects precipitation efficiency. Another important finding is that the response of precipitation extremes to warming may be related to changes in convective organization. Again in idealized RCE simulations with

homogeneous boundary conditions and no rotation, tropical convection has been shown to be able to spontaneously organize into a large convective cluster, which is referred to as convective self-aggregation (Held et al., 1993; Bretherton et al., 2005; Wing et al., 2018). The degree of organization in these studies can vary with changing setups and several studies found notable increases in precipitation extremes when convection becomes more aggregated (Bao et al., 2017; Pendergrass et al., 2016; Fildier et al., 2020). Bao and Sherwood (2019) showed that daily precipitation extremes increase in a more organized state because organization increases the precipitation duration while instantaneous precipitation extremes are almost not affected. Fildier et al. (2020) found that organization intensifies hourly precipitation extremes by increasing precipitation efficiency. One major concern of these studies is the small domain and the simple idealization adopted in RCE. As a result, processes occurring at scales that are beyond the limit of the domain size are missing.

In this study, we use a realistically configured global storm-resolving model to investigate the role of microphysics in tropical precipitation extremes. Similar to Parodi and Emanuel (2009), the microphysical element we focus on is the terminal velocity of raindrops. As the simulation covers a global domain, large-scale circulation and its impact on tropical convection and precipitation extremes are included. Additionally, we expect that the microphysical processes, despite happening at convective scales, may feed back to larger scales. The rest of the article is organized as follows: section 2 describes model details and experiments, section 3 shows results, and our discussion and conclusions are given in section 4.

2 Model and experiments

The simulations are conducted with ICON (Icosahedral Nonhydrostatic Weather and Climate Model; Zängl et al., 2015) at a quasi-uniform horizontal mesh of 5 km. The experiments are configured following the experimental protocol for DYAMOND (The DYnamics of the Atmospheric general circulation Modeled On Non-hydrostatic Domains; Stevens et al., 2019), in which the global meteorological analysis from the European Center for Medium Range Weather Forecasts (ECMWF) are used to initialize the model and daily observed sea surface temperatures are forced as boundary conditions. All the simulations are run for 20 days from August 1st in 2016, and the hourly output for the last 5 days over the tropical ocean grids (30°N-10°S) are used in the analysis.

The microphysics scheme (Baldauf et al., 2011) used has five hydrometeor species (rain, snow, graupel, cloud ice and cloud water). It is a single-moment scheme in which the precipitation particles are assumed to be exponentially distributed in size with respect to particle diameter. The terminal velocity of individual raindrops in this scheme is assumed to be only related to drop size. We change the terminal velocity of raindrops (V_{rain}) by rescaling the original formula with a fixed coefficient (Table 1), including a control simulation with the default V_{rain} (Ct), an increased velocity simulation with doubled V_{rain} (Db), and two decreased velocity simulations with quartered V_{rain} (Qt) and halved V_{rain} (Hf). The microphysical process is perturbed in an extreme way to investigate the impact. Unlike Parodi and Emanuel (2009) who adopted a fixed velocity for all raindrops, our method perturbs the relative magnitude of the fall speed and, thus, should not substantially alter the particle interactions. The other physical parameterizations include a radiation scheme (Rapid Radiative Transfer Model; Mlawer et al., 1997), a turbulent mixing scheme (Raschendorfer, n.d.) based on a prognostic equation for turbulent kinetic energy (TKE) and an interactive surface flux scheme and soil model (Schrodin & Heise, 2002). Further details about ICON and the DYAMOND configuration are given by Hohenegger et al. (2020).

Table 1. Acronyms of the experiments, the corresponding microphysical modifications to the terminal velocity of raindrops ($V_{rain}*$ rescaling coefficient), statistics of the convective organization metric I_{org} diagnosed from precipitable water (PW) and precipitation (PR), and the mean net atmospheric radiation for all-sky ($R_{a,total}$: W m^{-2}) and clear-sky ($R_{a,cs}$: W m^{-2}) conditions.

Name	Rescaling coefficient	I_{org}(PW)	I_{org}(PR)	$R_{a,total}$	$R_{a,cs}$
Qt	0.25	0.939	0.874	-98.3	-118.9
Hf	0.5	0.861	0.841	-105.2	-119.5
Ct	1.0	0.834	0.803	-109.0	-119.8
Db	2.0	0.829	0.806	-111.5	-120.7

3 Results

3.1 Thermodynamic characteristics of the tropical mean state

We first focus on some of the thermodynamic characteristics of the tropical mean state. Figure 1a and 1b show the differences in the virtual temperature (T_v) and relative humidity (RH) of the runs with modified terminal velocity relative to the control run (Ct). With a slower terminal velocity of raindrops, the troposphere becomes more stable as the free troposphere is substantially warmer, whereas the boundary layer is colder. Meanwhile, the entire troposphere becomes more humid especially between 600hPa and 800hPa. A cooler and moister boundary layer can be attributed to the slower raindrop velocity which increases the residence time of the raindrops and enhances evaporation (Fig. 1c). A warmer free troposphere can be explained from the changes in humidity, as the troposphere gets moister, it better protects rising convective parcels from the impact of entrainment, which, as a result, ensures a more precise moist-adiabatic ascent (Singh & O'Gorman, 2013; Seeley & Romps, 2015). Gravity waves then act to quickly adjust the temperature in the non-convective regions and homogenize the temperature horizontally in the free troposphere (Bretherton & Smolarkiewicz, 1989; Sobel & Bretherton, 2000). Thus, the tropical troposphere becomes warmer and more stable with a decreased raindrop velocity. On the other hand, an increased raindrop terminal velocity leads to the opposite response by reducing the residence time of the raindrops and suppressing evaporation, promoting a colder and less stable troposphere. Thus, the change in the microphysics which happens at small scales is shown to impact the tropics as a whole.

3.2 Tropical precipitation extremes

Fractional changes of precipitation as a function of precipitation percentile are shown in Figure 1d. Here we compare hourly and daily precipitation calculated from simulations with different raindrop terminal velocities relative to Ct. Extreme precipitation exhibits distinct variations at different time scales. At hourly time scales, extreme precipitation increases roughly linearly with the terminal velocity. At high precipitation percentiles (> 99.9th), precipitation reduces by 50% in Qt and 20% in Hf while increasing by ~20% in Db. On the other hand, daily precipitation extremes do not seem to vary linearly with the terminal velocity. The highest daily extremes occur in the case with the slowest terminal velocity (Qt), increasing by ~40% at 99.99th percentile. A dramatic change in extreme precipitation from hourly to daily time scales (especially in Qt) suggests they are potentially controlled by different mechanisms.

To better understand the mechanisms controlling extreme precipitation, we apply a scaling analysis method that separates extreme precipitation into thermodynamic, dynamic and precipitation efficiency components following O'Gorman and Schneider (2009)
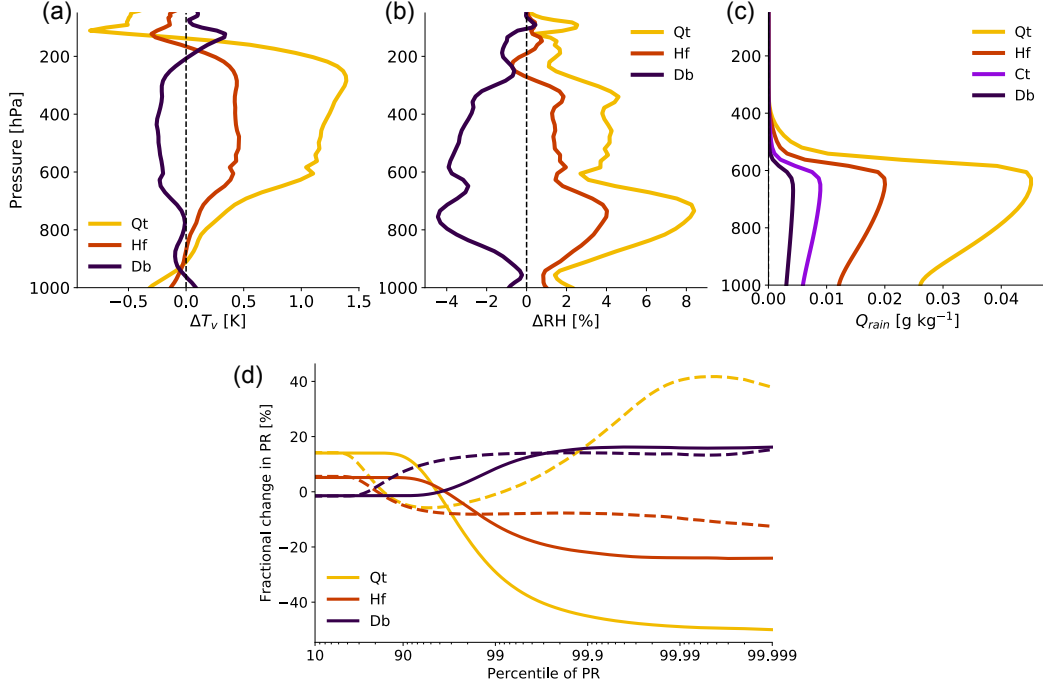
Figure 1. (a,b) Difference in tropical mean virtual temperature (T_v) and relative humidity (RH) relative to Ct. (c) Profiles of the tropical mean rain mixing ratio (Q_{rain}). (d) Fractional changes in precipitation (PR) relative to Ct as a function of PR percentile. Solid (dashed) lines represent hourly (daily) precipitation.

and Muller et al. (2011). First, a high-percentile precipitation rate (P_e) is represented by the product of net condensation rate (C) and precipitation efficiency (ϵ) conditioned on P_e:

$$P_e = \epsilon C. \tag{1}$$

The condensation rate can be approximated as:

$$C \approx \int_{p_s}^{p_t} \frac{\omega}{g} \frac{dq_s}{dp}\bigg|_{\theta_e^*} dp, \tag{2}$$

where p_s and p_t are pressure at the surface and the tropospause, g is the acceleration from gravity, ω is the updraft velocity in pressure coordinates conditioned on precipitation extremes, and $\frac{dq_s}{dp}\big|_{\theta_e^*}$ is the change in saturation specific humidity with respect to pressure at constant saturation equivalent potential temperature θ_e^* and is referred to as the moisture lapse rate. Eq. (2) assumes that condensation occurs roughly moist-adiabatically during an extreme precipitation event. The condensation here represents the net condensation (condensation minus evaporation). As a result, ϵ, differs from a conventional precipitation efficiency, is defined as the extreme precipitation rate divided by the net condensation rate. Following the steps in Fildier et al. (2020) (except using pressure coordinates here), we define a dynamical term (M) which represents the column-integrated mass flux as:

$$M = -\int_{p_s}^{p_t} \frac{\omega}{g} dp. \tag{3}$$

Then a thermodynamic term (Γ_q) dominated by the moisture lapse rate can be obtained by dividing the condensation rate by the dynamical term using Eq. (2),(3):

$$\Gamma_q \approx -\frac{1}{M} \int_{p_s}^{p_t} \frac{\omega}{g} \frac{dq_s}{dp}\bigg|_{\theta_e^*} dp = -\int_{p_s}^{p_t} \frac{1}{g} \frac{\omega}{M} \frac{dq_s}{dp}\bigg|_{\theta_e^*} dp. \tag{4}$$

Note that M is a single value and can be put inside the integral to separate the dynamical component from ω. By combining Eq. (1),(2),(3),(4), we have:

$$P_e \approx \epsilon M \Gamma_q. \tag{5}$$

Thus, changes in extreme precipitation can be decomposed into a dynamical component ($\frac{\delta M}{M}$) through changes in updraft velocity, a thermodynamic component ($\frac{\delta \Gamma_q}{\Gamma_q}$) through changes in the moisture lapse rate, and a precipitation efficiency component ($\frac{\delta \epsilon}{\epsilon}$):

$$\frac{\delta P_e}{P_e} \approx \frac{\delta \epsilon}{\epsilon} + \frac{\delta M}{M} + \frac{\delta \Gamma_q}{\Gamma_q} \tag{6}$$

3.2.1 Hourly precipitation extremes

At hourly time scales, changes in precipitation extremes are almost entirely due to the dynamical component while the thermodynamic and efficiency components play little role (Fig. 2). As the dynamical component is controlled by updraft velocity, it indicates that the convective updraft is stronger (weaker) when the terminal velocity is faster (slower). This is confirmed in Fig. 2g showing that the updraft velocity increases following the raindrop terminal velocity throughout the entire troposphere. One potential explanation for the increase in the updraft velocity is the reduced tropospheric stability, as section 3.1 shows that the troposphere becomes increasingly unstable with a faster raindrop terminal velocity. Another possibility is the weakened condensate loading effect resulting from more rapid removal of condensates from the atmosphere when raindrops are allowed to fall faster (Parodi & Emanuel, 2009). This tends to moderate the condensate loading effect in reducing the updraft buoyancy.

To separate these two effects and thus to understand what controls the updraft speed when hourly precipitation extremes occur, we investigate its relationship with buoyancy (B) as the vertically integrated buoyancy provides the kinetic energy for the convective updraft:

$$\frac{1}{2} w_{max}^2 \sim \int_0^{z_t} B \, dz, \tag{7}$$

where w_{max} is the maximum value of vertical velocity in the vertical column and z_t is fixed at about 11 km. The buoyancy of an updraft air parcel is formulated as:

$$B \approx g \frac{T_v'}{\overline{T}_v} - gl', \tag{8}$$

where T_v' is the virtual temperature excess between the updraft air parcel and its environment and l' is the rain water mixing ratio in the updraft column. The updraft grid cells are identified as the grid cells in which w_{max} exceeds the 99.9th percentile value. Then for each updraft, the corresponding environment is defined as the non-cloudy grid cells (the mixing ratio of the total condensates $< 10^{-5} \, \text{kg} \, \text{kg}^{-1}$) within 30 km radius of the updraft grid cell. The first term of on the right-hand side in Eq. (8) is associated with the static stability of the updraft environment, and the second term depicts the reduction of the updraft buoyancy from the condensate loading as the condensates increase the effective density of the updraft system. We can test the impact of condensate loading by comparing the relationship between the updraft kinetic energy and the vertical integration of the buoyancy with the buoyancy computed either including or omitting the loading term.
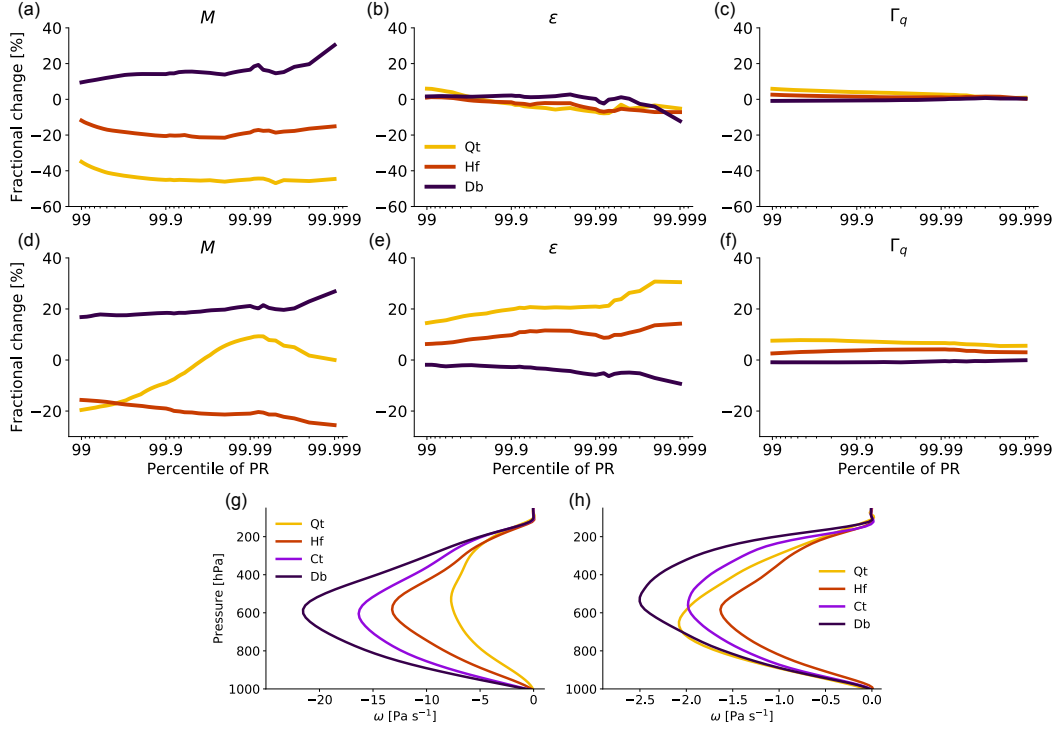
Figure 2. (Upper two rows) Fractional changes in the dynamical component (M), precipitation efficiency component (ϵ) and thermodynamic component (Γ_q) relative to Ct as a function of PR percentile. Results are shown for hourly (a-c) and daily (d-f) precipitation. (Lower row) Profiles of pressure velocity (ω) composited by 99.999th percentile of hourly (g) and daily (h) precipitation.

In Figure 3, we compare the updraft peak kinetic energy with the vertical integration of the buoyancy one excluding (Fig. 3a) and one including the condensate loading term (Fig. 3b). By including the condensate loading term, the updraft peak kinetic energy is much better correlated with the buoyancy integral, with the Pearson correlation coefficient (R) increasing from 0.46 to 0.73. This implies that the change in the condensate loading caused by varying raindrop terminal velocity is crucial to modulating the updraft buoyancy and thus also the updraft speed. Therefore, hourly precipitation extremes are mostly determined by the dynamical contribution from changes in the convective updraft, and the updraft speed is sensitive to microphysics through the condensate loading effect, in agreement with the results of Parodi and Emanuel (2009).

3.2.2 Daily precipitation extremes

For daily precipitation extremes, the dynamical component still plays a very important role as it contributes to the highest percentiles (99.999th) roughly 20% increase in Db and 20% reduction in Hf (Fig. 2d). However, in Qt where the dramatic rise in precipitation extremes occur, contributions from both the dynamics and efficiency are important (Fig. 2e). While the precipitation efficiency always favors intensifying extremes in Qt, the dynamical component shifts from negative contributions at less extreme (<99.95th) percentiles to positive contributions at more extreme percentiles. Finally, the thermodynamic component is mainly associated with the slight temperature changes, and con-
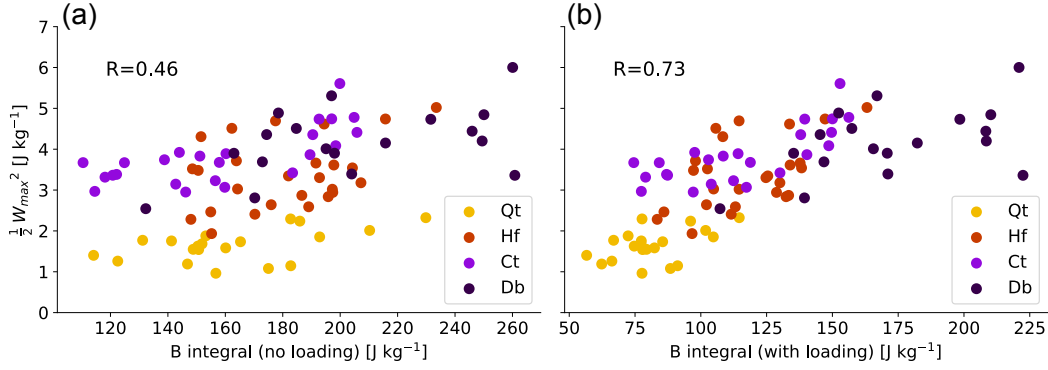
Figure 3. Peak kinetic energy ($\frac{1}{2}w_{max}{}^2$) vs. vertical integrated buoyancy (B) calculated without the loading effect (a) and with the loading effect (b).

sistent with its role at hourly time scales, its contribution to daily extremes is also less important than the other two components (Fig. 2f).

Figure 2e also shows that precipitation efficiency is negatively correlated with the raindrop terminal velocity. For the highest (99.999th) percentile, efficiency increases by $\sim$30% in Qt and $\sim$10% in Hf while reducing by $\sim$10% in Db. In idealized RCE simulations, higher precipitation efficiency often occurs in the state of more organized convection (Bao & Sherwood, 2019; Fildier et al., 2020). We believe this conclusion also holds here and that the degree of convective organization plays a role in the daily precipitation extremes. To explore the impact of organization, first we plot the probability density functions of RH. Figure 4 shows bimodal structures of the RH distributions with distinct moist and dry peaks in all cases. The bimodality is most pronounced in Qt, and becomes less pronounced with increasing raindrop velocity. As an increased moisture variance is a typical feature of more organized convection (Wing et al., 2018), Fig. 4 suggests that convection is the most organized in Qt. To complement this qualitative interpretation, we quantify the degree of organization with the organization index I_{org} (Table 1), which is based on the distribution of the nearest neighbor distance between identified convective clusters (Tompkins & Semie, 2017). We identify the grid cells where the precipitable water (PW) exceeds the 99.9th percentile value as convective grid cells. Two convective grid cells belong to one convective cluster if they share one boundary. The calculation of I_{org} using PW is referred to as I_{org}(PW). To test the robustness of the results, we also apply the same calculation, but using daily precipitation data to identify convective clusters I_{org}(PR). As a higher I_{org} indicates more organized convection, the result, consistent with Fig. 4, reveals that Qt, which has the highest precipitation efficiency, is the most organized, and the degree of organization decreases with increasing raindrop terminal velocity. At daily time scales, precipitation efficiency is mainly affected by the horizontal advection of water (Muller et al., 2011). In a more organized state, more moisture is transported to the column where extreme precipitation occurs. In addition to increasing precipitation efficiency, more organized convection can induce precipitation events to last longer, exerting positive dynamical contribution. This is especially the case of Qt in which multiple tropical cyclones develop. Despite having the weakest updraft speed at hourly time scales, organization intensifies the mean updraft averaged over a day by being more persistent in the same locations.

We speculate that the varying degrees of organization here is related to the changes in the atmospheric cloud radiative effect (ACRE) and the surface enthalpy fluxes. For ACRE, as discussed in section 3.1, when the terminal velocity is greater, the troposphere becomes drier. Thus, the clouds tend to shrink and the cloud radiative effect is weak-
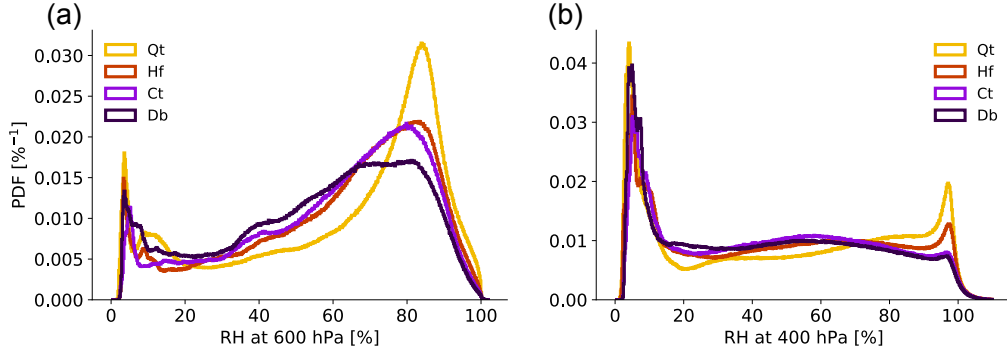
Figure 4. Probability density functions (PDF) of relative humidity (RH) distribution at 600 hPa (a) and 400 hPa (b).

ened. Indeed, the net atmospheric radiation under the clear-sky conditions changes little among the simulations, while it differs substantially under the all-sky conditions (Table 1), contributed mostly by the changes in the outgoing longwave radiation. As the difference in the net atmospheric radiation between the all-sky and the clear-sky conditions represents the cloud radiative effect, it implies that the strength of ACRE reduces with increasing terminal velocity. Such differences in ACRE, driven by the changes in the microphysics, develop very rapidly during the first few days of the simulations. They influence the net atmospheric energy uptake which, as a result, modulate the mean circulation and organization. This result is consistent with Popp and Bony (2019) who also found that the cloud radiative effect affects the zonal convective clustering in observation. In terms of the surface fluxes, when the terminal velocity is reduced, increased evaporation favors stronger cold pools which lead to enhanced surface fluxes. This, through a wind-induced surface heat exchange (WISHE) feedback, also contributes to a more organized state. Such a feedback is especially important in Qt where multiple tropical cyclones develop, as the feedback between surface wind and surface enthalpy flux are very fundamental for tropical cyclones (Zhang & Emanuel, 2016; Muller & Romps, 2018).

In contrast to hourly precipitation extremes that are mainly determined by the convective-scale dynamics, microphysics affects daily extremes by changing the behavior of organization over larger scales. A more organized state primarily increases the precipitation efficiency while at the same time can lead to a more positive dynamical contribution by intensifying the updraft speed.

4 Discussion and conclusions

We use a global storm-resolving model to investigate the impact of microphysics (terminal velocity of raindrops) on tropical precipitation extremes. We find that the microphysics influences hourly precipitation extremes by changing the convective updraft speed, which is fundamentally linked to the condensate loading effect dictated by the raindrop terminal velocity in the microphysics parameterization. Contrarily, daily precipitation extremes are related to the microphysical influence on convective organization, as organization enhances daily precipitation extremes by higher precipitation efficiency and intensified updrafts.

This work highlights the importance of microphysics in tropical precipitation extremes over different time scales. First it shows the dependence of convective updraft speed on raindrop terminal velocity, emphasizing the often overlooked microphysical mod-

ulation on convective-scale dynamics as first proposed by Parodi and Emanuel (2009). Further, it demonstrates that changes in small-scale microphysics can influence the mean climate as a whole. In particular, the microphysical imprints on convective organization can modulate precipitation extremes accumulated over long time scales, confirming the results from idealized RCE simulations that daily precipitation extremes increase when convection becomes more organized (Bao & Sherwood, 2019).

This work confirms, in a realistic simulation, the possibility of having varying degrees of convective organization, as is often reported in idealized simulations of RCE. Typical impacts of having convection being more organized, such as increased moisture variances and enhanced precipitation efficiency, are in line with the results obtained from those RCE simulations. The different behavior of convective organization is linked to the microphysical modulation on moisture, which influences the cloud radiative effect and the surface flux feedbacks. This supports the conclusions from idealized RCE simulations that the radiative feedbacks and surface flux feedbacks are important for convective organization (Wing et al., 2018).

The fundamental role of microphysics lies in its modification of moisture. Although the microphysical element explored in this work is the terminal velocity of raindrops, many other microphysical parameters can lead to similar changes. Thus, the results in this work should serve as an example to illustrate the non-negligible role of microphysical processes in affecting the tropical climate over a range of scales. To better simulate the tropical climate especially the precipitation extremes, an improved understanding of its interaction with the microphysics is hence desired.

References

Allen, M. R., & Ingram, W. J. (2002). Constraints on future changes in climate and the hydrologic cycle. *Nature*, *419*(6903), 228-232. doi: 10.1038/nature01092

Baldauf, M., Seifert, A., Förstner, J., Majewski, D., Raschendorfer, M., & Reinhardt, T. (2011). Operational convective-scale numerical weather prediction with the cosmo model: Description and sensitivities. *Monthly Weather Review*, *139*(12), 3887-3905. doi: 10.1175/mwr-d-10-05013.1

Bao, J., & Sherwood, S. C. (2019). The role of convective self-aggregation in extreme instantaneous versus daily precipitation. *Journal of Advances in Modeling Earth Systems*, *11*(1), 19-33. doi: 10.1029/2018ms001503

Bao, J., Sherwood, S. C., Colin, M., & Dixit, V. (2017). The robust relationship between extreme precipitation and convective organization in idealized numerical modeling simulations. *Journal of Advances in Modeling Earth Systems*, *9*(6), 2291-2303. doi: https://doi.org/10.1002/2017MS001125

Bretherton, C. S., Blossey, P. N., & Khairoutdinov, M. (2005). An energy-balance analysis of deep convective self-aggregation above uniform sst. *Journal of the Atmospheric Sciences*, *62*(12), 4273-4292. doi: 10.1175/JAS3614.1

Bretherton, C. S., & Smolarkiewicz, P. K. (1989). Gravity waves, compensating subsidence and detrainment around cumulus clouds. *Journal of the Atmospheric Sciences*, *46*(6), 740-759. doi: 10.1175/1520-0469(1989)046⟨0740:GWCSAD⟩2.0

.CO;2

Fildier, B., Collins, W. D., & Muller, C. (2020). Distortions of the rain distribution with warming, with and without self-aggregation. *Journal of Advances in Modeling Earth Systems*, *n/a*(n/a), e2020MS002256. doi: https://doi.org/10.1029/2020MS002256

Held, I. M., Hemler, R. S., & Ramaswamy, V. (1993). Radiative-convective equilibrium with explicit two-dimensional moist convection. *Journal of Atmospheric Sciences*, *50*(23), 3909-3927. doi: 10.1175/1520-0469(1993)050⟨3909:RCEWET⟩2.0.CO;2

Held, I. M., & Soden, B. J. (2006). Robust responses of the hydrological cycle to global warming. *Journal of Climate*, *19*(21), 5686-5699. doi: 10.1175/JCLI3990.1

Hohenegger, C., Kornblueh, L., Klocke, D., Becker, T., Cioni, G., Engels, J. F., ... Stevens, B. (2020). Climate statistics in global simulations of the atmosphere, from 80 to 2.5 km grid spacing. *Journal of the Meteorological Society of Japan. Ser. II*, *98*(1), 73-91. doi: 10.2151/jmsj.2020-005

Mlawer, E. J., Taubman, S. J., Brown, P. D., Iacono, M. J., & Clough, S. A. (1997). Radiative transfer for inhomogeneous atmospheres: Rrtm, a validated correlated-k model for the longwave. *Journal of Geophysical Research: Atmospheres*, *102*(D14), 16663-16682. doi: 10.1029/97jd00237

Muller, C. J., O'Gorman, P. A., & Back, L. E. (2011). Intensification of precipitation extremes with warming in a cloud-resolving model. *Journal of Climate*, *24*(11), 2784-2800. doi: 10.1175/2011JCLI3876.1

Muller, C. J., & Romps, D. M. (2018). Acceleration of tropical cyclogenesis by self-aggregation feedbacks [Journal Article]. *Proceedings of the National Academy of Sciences*, *115*(12), 2930. doi: 10.1073/pnas.1719967115

O'Gorman, P. A., & Schneider, T. (2009). The physical basis for increases in precipitation extremes in simulations of 21st-century climate change. *Proceedings of the National Academy of Sciences*, *106*(35), 14773. doi: 10.1073/pnas.0907610106

O'Gorman, P. A. (2015). Precipitation extremes under climate change. *Current Climate Change Reports*, *1*(2), 49-59. doi: 10.1007/s40641-015-0009-3

Parodi, A., & Emanuel, K. (2009). A theory for buoyancy and velocity scales in deep moist convection. *Journal of the Atmospheric Sciences*, *66*(11), 3449-3463. doi: 10.1175/2009JAS3103.1

Pendergrass, A. G., Reed, K. A., & Medeiros, B. (2016). The link between extreme precipitation and convective organization in a warming climate: Global radiative-convective equilibrium simulations. *Geophysical Research Letters*, *43*(21), 11,445-11,452. doi: 10.1002/2016GL071285

Popp, M., & Bony, S. (2019). Stronger zonal convective clustering associated with a wider tropical rain belt. *Nature Communications*, *10*(1), 4261. doi: 10.1038/s41467-019-12167-9

Raschendorfer, M. (n.d.). The new turbulence parameterization of lm. *COSMO Newsletter*(1), 89–97. doi: 10.1038/s41467-019-12167-9

Schrodin, R., & Heise, E. (2002). A new multi-layer soil model. *COSMO Newsletter*(2), 149-151.

Seeley, J. T., & Romps, D. M. (2015). Why does tropical convective available potential energy (cape) increase with warming? *Geophysical Research Letters*, *42*(23), 10,429-10,437. doi: 10.1002/2015GL066199

Singh, M. S., & O'Gorman, P. A. (2013). Influence of entrainment on the thermal stratification in simulations of radiative-convective equilibrium. *Geophysical Research Letters*, *40*(16), 4398-4403. doi: 10.1002/grl.50796

Singh, M. S., & O'Gorman, P. A. (2014). Influence of microphysics on the scaling of precipitation extremes with temperature. *Geophysical Research Letters*, *41*(16), 6037-6044. doi: 10.1002/2014GL061222

Sobel, A. H., & Bretherton, C. S. (2000). Modeling tropical precipitation in a single column. *Journal of Climate*, *13*, 4378-4392. doi: 10.1175/1520-0442(2000) 013⟨4378:MTPIAS⟩2.0.CO;2

Stevens, B., Satoh, M., Auger, L., Biercamp, J., Bretherton, C. S., Chen, X., . . . Zhou, L. (2019). Dyamond: the dynamics of the atmospheric general circulation modeled on non-hydrostatic domains. *Progress in Earth and Planetary Science*, *6*(1), 61. doi: 10.1186/s40645-019-0304-z

Tompkins, A. M., & Semie, A. G. (2017). Organization of tropical convection in low vertical wind shears: Role of updraft entrainment. *Journal of Advances in Modeling Earth Systems*, *9*(2), 1046-1068. doi: 10.1002/2016MS000802

Wing, A. A., Emanuel, K., Holloway, C. E., & Muller, C. (2018). Convective self-aggregation in numerical simulations: A review. In R. Pincus, D. Winker, S. Bony, & B. Stevens (Eds.), *Shallow clouds, water vapor, circulation, and climate sensitivity* (p. 1-25). Cham: Springer International Publishing. doi: 10.1007/978-3-319-77273-8_1

Zhang, F., & Emanuel, K. (2016). On the role of surface fluxes and wishe in tropical cyclone intensification. *Journal of the Atmospheric Sciences*, *73*(5), 2011-2019. doi: 10.1175/JAS-D-16-0011.1

Zängl, G., Reinert, D., Rípodas, P., & Baldauf, M. (2015). The icon (icosahedral non-hydrostatic) modelling framework of dwd and mpi-m: Description of the non-hydrostatic dynamical core. *Quarterly Journal of the Royal Meteorological Society*, *141*(687), 563-579. doi: 10.1002/qj.2378